Photochemical & Photobiological Sciences

PAPER

A light-regulated bZIP module, Photozipper, induces the binding of fused proteins to the target DNA sequence in a blue light-dependent manner†

O. Hisatomi[a,*] and K. Furuya[a]

Aureochrome-1 (AUREO1) has been identified as a blue light (BL) receptor responsible for the BL-induced blanching of a stramenopile alga, *Vaucheria frigida*. BL induces the dimerization of monomeric AUREO1, which subsequently increases its affinity for the target sequence. We made a synthetic gene encoding N-terminally truncated monomeric AUREO1 (Photozipper protein) containing a basic region/leucine zipper (bZIP) domain and a light-oxygen-voltage-sensing domain. In the present study, yellow fluorescent protein or mCherry protein was fused with the Photozipper (PZ) protein, and their oligomeric structures and DNA-binding were compared in the dark and light states. Dynamic light scattering and size exclusion chromatography demonstrated that the hydrodynamic radii and molecular masses of the fusion proteins increased upon BL illumination, suggesting that fusion PZs underwent BL-induced dimerization. Moreover, BL-induced dimerization enhanced their affinities for the target sequence. Taken together, PZ likely functions as a BL-regulated bZIP module in fusion proteins, and can possibly provide a new approach for controlling bZIP transcription factors.

Introduction

The light-oxygen-voltage-sensing (LOV) domains are present in many signaling proteins in bacteria, archaea, protists, plants, and fungi. A group of LOV domains noncovalently bind with flavin mononucleotide (FMN) and play roles in the recognition of blue light (BL). Examples include phototrophin,[1] the LOV-F box-kelch repeat protein families (ZTL, LKP2, and FKF1),[2] a LOV-STAS (sulfate transporter and anti-sigma antagonist) protein (YtvA),[3] and LOV-histidine kinase (HK) proteins.[4-6] In these proteins, BL absorbed by FMN induces the formation of a covalent adduct with a highly conserved cysteine residue in the LOV domain.[7-9] This photochemical reaction further induces conformational changes of the LOV domain, and alters the intramolecular interactions with effecter domains and/or the intermolecular interactions with other proteins. These light-induced changes of LOV domains have recently been used as optogenetic tools to control intracellular signal transductions, as well as cellular activities and organizations.[10-19]

LOV proteins with a DNA-binding domain have been found in stramenopiles,[20,21] *Neurospora*,[22] and a marine bacterium.[23] Aureochrome (AUREO) was first identified as a BL receptor in a stramenopile alga, *Vaucheria frigida*.[20] Its two homologs named aureochrome-1 (AUREO1) and aureochrome-2 have been reported to play roles in BL-induced branching and

development of a sex organ, respectively.[20] AUREOs consist of a LOV domain in the C-terminal region and a basic region/leucine zipper (bZIP) domain on the N-terminal side of the LOV domain. The bZIP domain is an α-helical DNA-binding motif found among eukaryotic transcription factors.[24] Recombinant AUREO1 bound to the target sequence TGACGT in a light-dependent manner, implying that the AUREO proteins function as BL-regulated transcription factors.[20]

By using a transient grating technique and size exclusion chromatography (SEC), Toyooka *et al.* (2011) reported that AUREO1-LOV was in a monomer-dimer equilibrium in the dark, and dimerized upon photoexcitation.[25] Based upon circular dichroism (CD) spectroscopy, BL appeared to reduce the α-helical content of the LOV domain.[26] The N-terminally truncated AUREO1 (ZL) consisting of the bZIP and LOV domains was in a dimeric form, connected through intermolecular disulfide linkages at C162 and C182, with a midpoint oxidation-redox potential (ORP) of approximately -245 ± 15 mV.[27] Dynamic light scattering (DLS) and SEC analyses showed that dithiothreitol (DTT)-treated ZL and a site-directed ZL mutant (ZLC2S), in which C162 and C182 were replaced with Ser, were monomeric in the dark. BL induced the dimerization of monomeric AUREO1s, which subsequently increased their affinity for the target sequence.[27] We therefore synthesized an optogenetically optimized gene (opZL) encoding the N-terminally truncated monomeric AUREO1-ZLC2S (designated as Photozipper protein).

In the present study, we also prepared four kinds of fusion proteins, in which yellow fluorescent protein (YFP) or mCherry (mCh) was fused at the N- or C-terminus of the Photozipper (PZ) protein. Spectroscopic, DLS, and SEC analyses

a. *Department of Earth and Space Science, Graduate School of Science, Osaka University, Toyonaka, Osaka 560-0043, Japan.*

* Correspondence: *hisatomi@ess.sci.osaka-u.ac.jp*

This journal is © The Royal Society of Chemistry 20xx

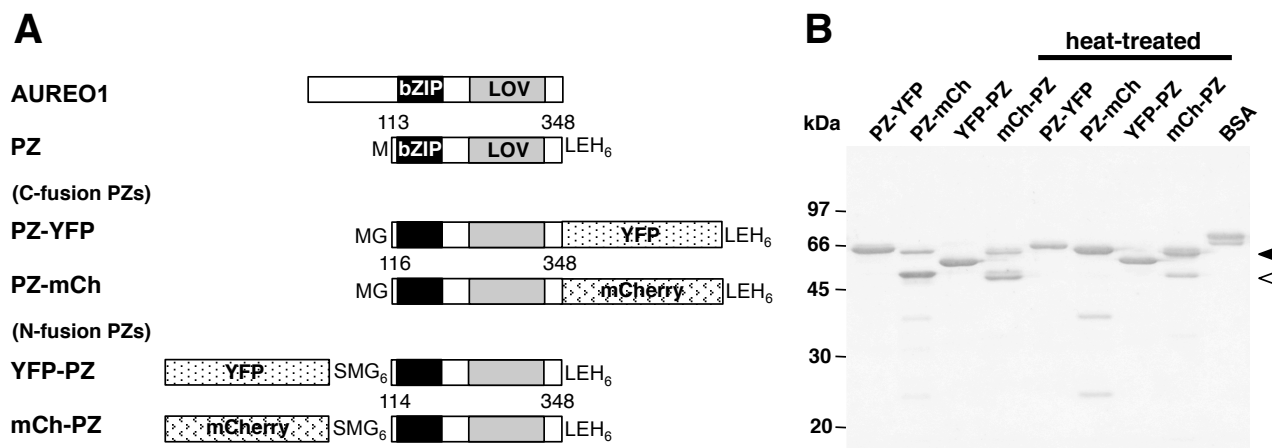*Photochem. Photobiol. Sci.*, 2015, **00**, 1-6 | **1**

Fig. 1 (A) Schematic drawing of recombinant PZ and fusion PZs, PZ-YFP, PZ-mCh, YFP-PZ, and mCh-PZ. The amino acid numbering is based on full-length AUREO1. (B) SDS-PAGE patterns of purified fusion PZs (1 µg in each lane) without (left) or with (right) heat treatment at 80ºC for 5 min, and BSA (1 µg). Open and closed arrowheads indicate the 54 kDa and 64 kDa species of mCh-fused PZs, respectively.

demonstrated that BL induced the dimerization of all fusion proteins, and subsequently increased their affinity for the target sequence. PZ functioned as a BL-regulated bZIP module in the fusion proteins, and may therefore provide a new approach for controlling bZIP transcription factors.

Results

Recombinant PZ proteins

Fig. 1A shows a schematic drawing of PZ and four kinds of fusion proteins (PZ-YFP, PZ-mCh, YFP-PZ, and mCh-PZ) used in this study. All fusion PZs contained a histidine hexamer tag (LEHHHHHH) at their C-termini, and a glycine hexamer (Gly6) was used as a linker for N-fusion PZs (YFP-PZ and mCh-PZ). The MW of each recombinant PZ calculated from the amino acid sequence was 54-55 kDa. Fig. 1B shows the SDS-PAGE patterns of purified fusion PZs (1 µg in each lane) with or without heat treatment. YFP-fused PZs appear as single bands of 60-65 kDa, whereas multiple bands are detected for mCh-fused PZs as shown for other mCh-fused proteins.[28] When mCh-fused PZs in SDS sample buffer solutions were heated to 80°C for 5 min, the major band shifted from approximately 54 kDa (open arrowhead) to 64 kDa (closed arrowhead), and minor bands of about 41 kDa and 23 kDa increased for PZ-mCh. Multiple bands of mCh-fused PZs were probably caused by the partial denaturation of the tertiary structure and degradation during SDS-PAGE procedures. Band intensity of each fusion PZ appeared to be comparable to that of 1 µg bovine serum albumin (BSA).

Absorption and fluorescence emission spectra

The absorption spectra of fusion PZs in the dark state (thick solid lines), just after BL illumination (dashed lines), and the spectral change during dark regeneration (thin solid lines), and 48 min after illumination (dotted lines) are shown in Fig. 2A-D (upper panels), with the normalized fluorescence emission spectra measured with excitations at 510 nm (for YFP-fused PZs) or 570 nm (for mCh-fused PZs) in gray lines. The λ_{max} of YFP- and mCh-fused PZs were 514 nm and 586 nm, respectively, which were almost identical to those of EYFP (513 nm) and mCh (587 nm). The spectral differences during dark regeneration (Fig. 2A-D, lower panels) show λ_{max} at 450 ± 1 nm, that was almost identical to that of AUREO1 with λ_{max} at 449 ± 1 nm.[26,27] The emission spectra of YFP-fused PZs show the same λ_{max} (527 nm) as that of EYFP, whereas mCh-fused PZs had blue shift emission maxima at 605-606 nm (emission maximum of mCherry was 610 nm). Fig. 2E shows the superimposition of time courses for the regeneration reactions of these recombinant PZs monitored at 450 nm. The half-life times ($\tau_{1/2}$) of the reactions were calculated as 7.3 ± 7.9 min, which was in agreement with those of ZLC2S ($\tau_{1/2} = 7.3 \pm 0.5$ min).[27] The spectroscopic properties of fluorescent proteins and photoreaction of LOV domains appeared to be intact in these fusion proteins. Assuming that molar extinction coefficients of YFP at 513 nm and mCh at 587 nm were 84,000 and 72,000 M^{-1} cm^{-1}, respectively, the concentrations of fluorescent proteins were estimated to be approximately 2.4 µM for YFP-fused PZs and 1.6-1.8 µM for mCh-fused PZs. Based upon the SDS-PAGE patterns and upon the absorption spectra, at least 60% of PZ and the fluorescent proteins appeared to be functional in these fusion PZs.
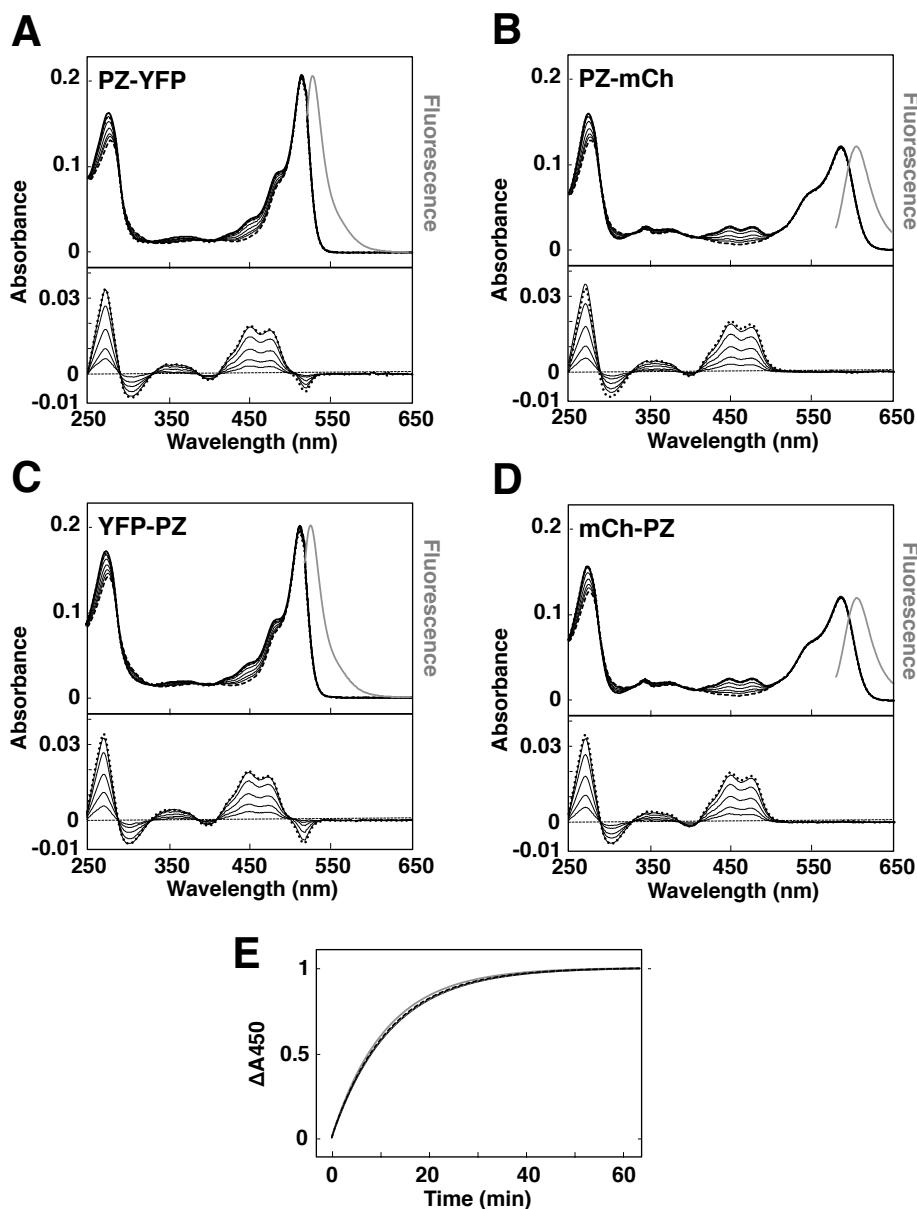
Fig. 2 Spectroscopic properties of (A) PZ-YFP, (B) PZ-mCh, (C) YFP-PZ, and (D) mCh-PZ. Absorption spectra in the dark state (thick solid lines), just after BL illumination (dashed lines), and the spectral change during dark regeneration (thin solid lines), and 48 min after illumination (dotted lines) are shown, with the normalized fluorescence emission spectra (gray lines) measured with excitations at 510 nm (for YFP fusion PZs) or 570 nm (for mCherry fusion PZs) in gray lines (upper panels). Lower panels, dark regeneration of absorption spectra after illumination. (E) Surperimposition of the normalized fitting curves of the dark regeneration time course for PZ-YFP (gray dashed line), PZ-mCh (black dashed line), YFP-PZ (gray solid line), and mCh-PZ (black solid line), using the formula, $\Delta A_{max}(1-e^{-kt})$, where ΔA_{max} is the maximum absorption difference and k is the rate constant of the reaction.

DLS analyses of recombinant PZs

The apparent hydrodynamic radii [$R_{H(app)}$] of fusion PZs were measured by DLS (Fig. S1). The $R_{H(app)}$ of PZ-YFP (Fig. 3A), PZ-mCh (Fig. 3B), YFP-PZ (Fig. 3C), and mCh-PZ (Fig. 3D) in dark (solid line), light (dashed line), and light-dark (dotted line) states depended in an approximate linear fashion on the protein concentrations (5-8 μM) because of interparticle and hydrodynamic interactions.[26,27,29] The R_H value for each fusion PZ was therefore determined by extrapolating $R_{H(app)}$ to a protein concentration of zero. Fusion PZs had an R_H from 3.4-3.9 nm in the dark state that increased to 4.3-4.5 nm after BL illumination (Table 1). When illuminated PZ solutions were kept in the dark for 1 h (the light-dark state), the R_H returned to the dark state values. The 15-26% changes in R_H between the dark and light states corresponded to a 52-100% increase in volume. The increments in R_H of fusion PZs were comparable to the 23% increase of ZLC$_2$S, primarily due to the dimerization of ZLC$_2$S.[27]

This journal is © The Royal Society of Chemistry 20xx

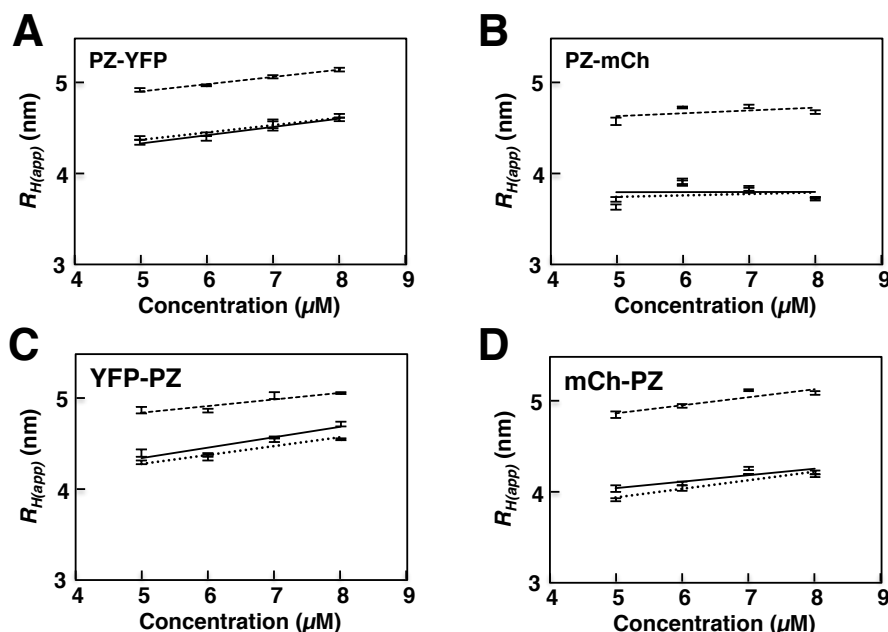*Photochem. Photobiol. Sci.*, 2015, **00**, 1-6 | **3**

Fig. 3 Dependence of $R_{H(app)}$ on the concentrations of (A) PZ-YFP, (B) PZ-mCh, (C) YFP-PZ, and (D) mCh-PZ, in the dark state (a thin solid line), the light state (a dashed line), and light-dark state (a dotted line), with SDs obtained from at least six measurements.

SEC measurements of fusion PZs

To verify the oligomeric structures, we carried out SEC analyses of fusion PZs at a protein concentration of 2 μM. Fig. 4 shows the elution profiles of PZ-YFP (Fig. 4A), PZ-mCh (Fig. 4B), YFP-PZ (Fig. 4C), and mCh-PZ (Fig. 4D) in the dark state (solid lines). The MWs estimated from the elution peaks at 13.7-13.8 mL (71-74 kDa) were larger than those of fusion PZs calculated from the amino acid sequence (Fig. 4E), probably because of their nonspherical shapes.[26,27] In the light state (dashed lines), the elution peaks shifted to the left to approximately 12.6 mL. The estimated MWs of each fusion PZ in the light state (117-123 kDa) were 1.5-1.7 times larger than those in the dark state, and comparable with those of their dimeric forms calculated from the sequence. The elution peaks of fusion PZs returned to the initial times in the light-dark state. The elution profiles of fusion PZs were basically unaffected when the NaCl concentration of the SEC buffer was reduced to

230 mM (Fig. S2A and 2B). Taken together, the DLS and SEC results indicated that fusion PZs underwent reversible dimerization upon illumination.

DNA binding of fusion PZs

We then investigated the binding of fusion PZs with an Alexa647-labeled AUREO1-specific palindromic oligonucleotide (647-Apo, Table S1) containing the target sequence (Fig. 5). Gray, green, and red lines indicate the elution profiles monitored at 260 nm (for the detection of DNA and protein), 520 nm (for the detection of YFP and mCh), and 650 nm (for the detection of 647-Apo), respectively. The elution peaks at 19-20 mL found in the 260 nm profiles were from EDTA contained in the 647-Apo solution. In the dark state (upper panels), PZ-YFP and PZ-mCh eluted with peak volumes at 13.6-13.7 mL (Fig. 5A and 5B), which were almost identical to those for the DNA-free samples in the dark state (Fig. 4A and 4B). The 647-Apo separately eluted from the fusion proteins with the peak elution volume at approximately 14.8 mL, that was almost identical to that of 647-Apo in the absence of proteins (Fig S2C). In the light state (middle), peak elution volumes of fusion proteins shifted to the left, with the absorbance at 650 nm detected within the first peak, indicating the formation of the PZ dimer and Apo (PZ_2/Apo) complexes. When a mixture of C-fusion PZs and 647-Apo was kept in the dark for 1 h (lower), the first peaks returned to their initial sizes and 647-Apo signals were separately eluted from the proteins. These results suggested that BL-induced dimerization of C-fusion PZs led the formation of PZ_2/Apo complexes.

Table 1 R_H values estimated from DLS analyses.

		R_H (nm)	
	dark	**light**	**light-dark**
PZ-YFP	3.9	4.5	4.0
PZ-mCh	3.4	4.3	3.3
YFP-PZ	3.8	4.5	3.8
mCh-PZ	3.7	4.4	3.5

4 | *Photochem. Photobiol. Sci.*, 2015, **00**, 1-6

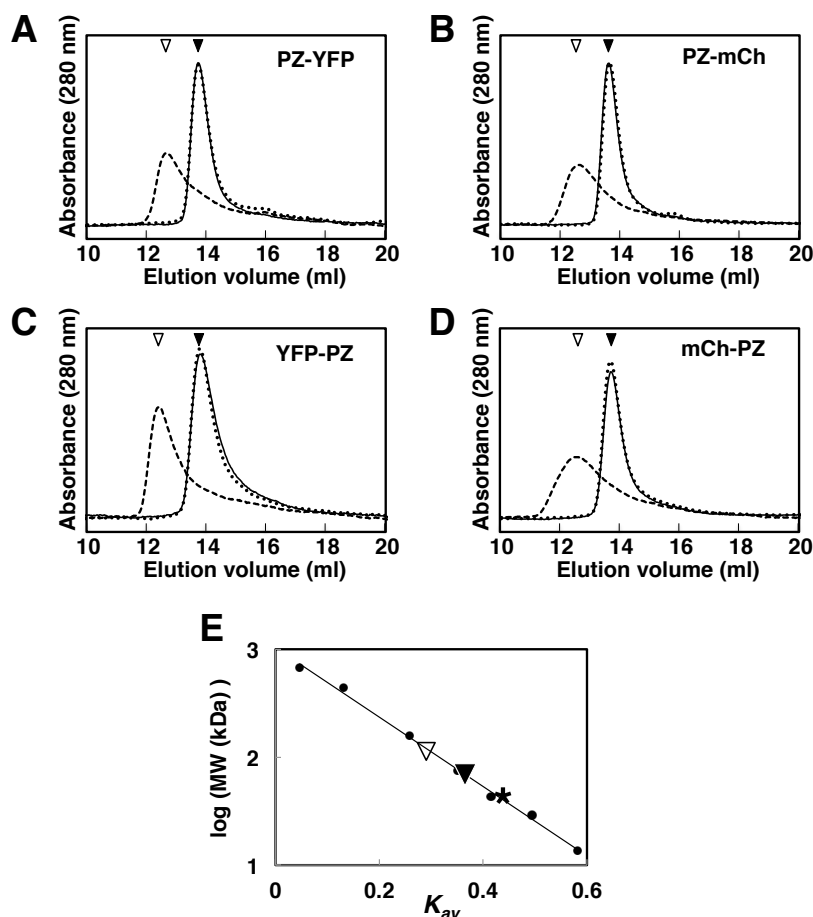This journal is © The Royal Society of Chemistry 20xx

Fig. 4 Elution profiles of (A) PZ-YFP, (B) PZ-mCh, (C) YFP-PZ, and (D) mCh-PZ in the dark state (thin solid lines), the light state (broken lines), and the light-dark state (dotted lines), monitored by their absorbance at 280 nm. (E) The MW estimated from the peak elution volumes of fusion PZs in the dark (closed inverted triangle) and light (open inverted triangle), and 647-Apo (asterisk). Circles indicate the MWs of the proteins used for column calibration.

In the case of N-fusion PZs, DNA binding was not detected, even in the light state when SEC buffer containing 300 mM NaCl was used (data not shown). The electrostatic interaction of the fluorescent proteins adjacent to the basic region probably interrupted its binding to DNA at high NaCl concentration.[26] We therefore reduced the NaCl concentration to 230 mM (Fig. 5C and 5D). In the dark and light-dark states (upper and lower), YFP-PZ and mCh-PZ separately eluted from 647-Apo with peak volumes at 13.6-13.7 mL. The elution peaks shifted to higher MWs at 12.4-12.5 mL, and 647-Apo co-eluted with the N-fusion PZs in the light state (middle). When Alexa647-labeled control palindromic oligonucleotide (647-Cpo) was used instead of 647-Apo, fusion PZ_2/Cpo complexes were not observed irrespective of the light conditions (Fig. S2D and S3A-D). The results suggested that both N- and C-fusion PZs bound to the target DNA sequence to form the PZ_2/Apo complex in a light-dependent manner as illustrated in Fig. 6, and that the affinity of fusion PZs for DNA could be modified by the amino acid sequences near the basic region.

Discussion

In the difference spectra of YFP-fused PZs during dark regeneration, negative bands with peak wavelengths at 520 nm were observed (Fig. 2A and 2C). No absorption band was detected for PZ at longer than 510 nm (Fig. S4A and S4B), suggesting that the negative bands were due to spectral difference of YFP moieties. When the spectral changes were subjected to the principle component analyses, the negative bands appeared in the first principle components with the positive bands of regenerated FMN at around 450 nm (Fig. S4C). The second principle components were small but also showed negative bands from 500-530 nm. The BL-induced dimerization of YFP-fused PZs possibly affected the surrounding electric field and modulated the absorbance of YFP.[30] Conformational change of YFP-fused PZs may be evaluated by these negative bands.

This journal is © The Royal Society of Chemistry 20xx

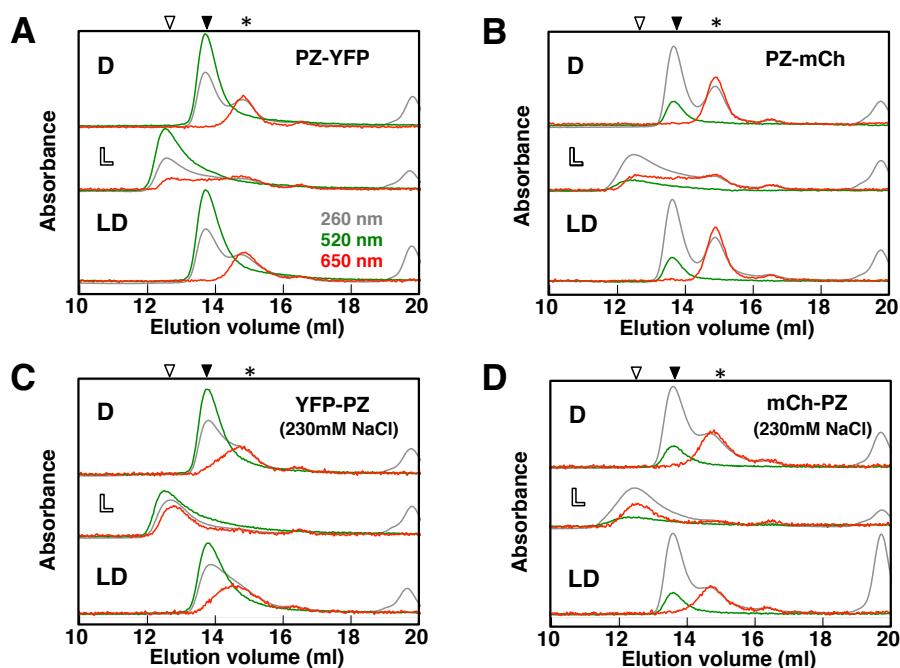*Photochem. Photobiol. Sci.*, 2015, **00**, 1-6 | **5**

Fig. 5 Elution profiles of (A) PZ-YFP, (B) PZ-mCh, (C) YFP-PZ, and (D) mCh-PZ incubated with 647-Apo in the presence of 300 mM (A and B) or 230 mM (C and D) NaCl, in the dark (D, upper), in the light (L, middle), and in the light-dark (LD, lower) states. Monitoring wavelengths were 260 nm (gray solid lines), 520 nm (green lines), and 650 nm (red lines). Inverted triangles indicate the peak elution volumes of fusion PZs in the dark (closed) and light (open) states, and asterisks designate the peak elution volume of double-stranded 647-Apo.

Recently, LOV domains with FMN chromophores have been used as optogenetic tools for controlling the activity of proteins and cells.[10-19] For example, using the FKF1 and GIGANTEA (GI) proteins of *Arabidopsis thaliana*, Yazawa *et al.* (2009) induced the local formation of lamellipodia in response to focal illumination.[11] They also generated a light-activated transcription factor by fusing domains of GI and FKF1 to the DNA-binding domain of Gal4 (Gal4-BD) and the transactivation domain of VP16 (VP16-AD), respectively. Wu *et al.* (2009) constructed photoactivatable Rac1 (PA-Rac1), in which Rac1 mutants were fused to the LOV domain, and showed that PA-Rac1 could be reversibly and repeatedly activated upon BL illumination to generate precisely localized cell protrusions and rufflings.[12] Strickland (2012) developed tunable light-inducible dimerization tags (TULIPs) based on a synthetic interaction between the AsLOV2 and an engineered PDZ domain, and showed that TULIPs could recruit proteins to diverse structures in living yeast and mammalian cells.[16] Most of these studies used in fusion-based design to generate synthetic light-activated hybrid proteins.[31] Thus, it was important to clarify the ability of PZ to function within the fusion protein. Because BL induced conformational changes of the bZIP domain and/or linker regions located at the N-terminal side of the LOV domain,[26,32] PZ was available for fusion proteins, in which only the N-fusion geometry was functional.

In addition to the conformational change of the Jα helix and the heterodimerization with other proteins or peptides, BL-induced homodimerization of LOV domains has been used to control protein activities. A light-switchable transactivator composed of Gal4-BD, the fungal photoreceptor Vivid (VVD), and VP16-AD (GAVP) have been developed and improved.[15,33] GAVP formed a dimer and bound promoters upon BL illumination, and rapidly induced transcription of target transgenes in mammalian cells and in mice. Recently, an engineered version of EL222, a bacterial LOV protein containing a helix-turn-helix DNA-binding domain, has been reported, which induced light-gated transcription in several mammalian cell lines and intact zebrafish embryos.[34] Kawano *et al.* (2015) reported multidirectional engineering of VVD to develop pairs of distinct photoswitches named Magnets.[35] Because incorporation of AUREO1-LOV resulted in robust activation of receptor tyrosine kinases by light-activated dimerization,[36] our PZ may be used as a dimerization module to regulate protein activities, including regulation of bZIP transcription factors.

Conclusions

6 | *Photochem. Photobiol. Sci.*, 2015, **00**, 1-6

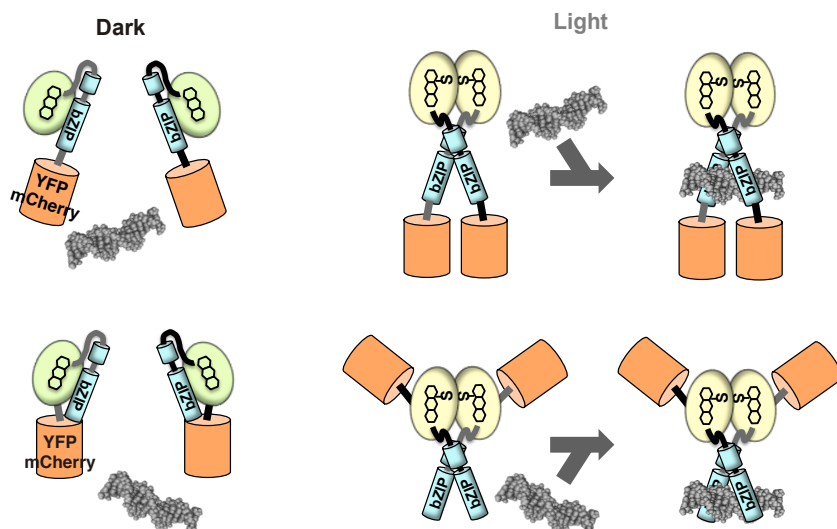This journal is © The Royal Society of Chemistry 20xx

Fig. 6 Schematic model of the oligomeric structures for N- and C-fused PZs. In the dark state, PZs existed as a monomer. BL induced dimerization of fusion PZs, which increased their affinity for the target DNA.

In the present study, we showed that all four fusion PZs underwent dimerization and subsequently increased their affinities for the target DNA in BL-dependent manners. The affinity could be modified by the amino acid sequence near the bZIP domain. Our PZ module may therefore provide a new approach for controlling bZIP transcription factors.

Experimental

Construction of expression vectors

An opZL gene encording G113-K348 of AUREO1 (PZ protein), in which C162 and C182 were replaced with serine and the codons were optimized for bacterial and mammalian expression, was synthesized (GeneScript) and inserted into a plasmid vector (pEopZL) as previously described.[24,25] To construct the expression vector for YFP-PZ (or mCh-PZ), the YFP (or mCh) gene in a plasmid vector was amplified with bPd/YFP-F (or bPd/mCh-F) and pET-ter-R primers (Fig. S1), fused with the amplified fragment of pEopZL using pET-ter-F and bPd/YFP-R (or bPd/mCh-R) primers for the in fusion cloning kit (Takara Bio), and two codons (S114 and I115) were deleted using pET-Pd-F and pET-Pd-R primers using a PrimeSTAR mutagenesis kit (Takara). To construct the expression vector for YFP-PZ (or mCh-PZ), the opZL gene was inserted between NcoI and XhoI sites of a plasmid vector pEYFPex (or pEmChex), and a glycine hexamer was added with bPdflxLinker-F and YFPflxLinker-R (or mChflxLinker-R) primers using the PrimeSTAR mutagenesis kit. Sequences of all constructs were confirmed using the Thermo Sequenase Dye Primer Manual Cycle Sequencing Kit (Affymetrix) with a SQ-5500 DNA sequencer (Hitachi Hi-Tech), and expression vectors of recombinant PZs were introduced into BL21 (DE3) cells (Invitrogen).

Purification of recombinant proteins

Recombinant PZ proteins were prepared as described previously.[24-26] In brief, *E. coli* cells expressing recombinant proteins were harvested by centrifugation and disrupted by sonication. After cell debris were removed by centrifugation, recombinant proteins were purified twice with a Ni-Sepharose[TM] 6 Fast Flow column (GE Healthcare) and a HiTrap Heparin HP column (GE Healthcare), according to the manufacturer's instructions. The recombinant proteins were stored at 4°C in the loading buffer (400 mM NaCl, 20 mM Tris-HCl, pH 7.0) containing 2 mM DTT and 0.2 mM PMSF. Each recombinant protein (1 µg) was denatured in sodium dodecylsulfate polyacrylamide gel electrophoresis (SDS-PAGE) sample buffer in the presence of 20 mM DTT, and subjected to SDS-PAGE analysis with crystallized BSA (Wako). Concentrations of the recombinant proteins were determined from the absorbance difference at 450 nm between dark and light states using 10,600 $M^{-1}cm^{-1}$ as the extinction coefficient.

Spectroscopic measurements

Recombinant proteins were diluted to 2 µM with the loading buffer, and ultraviolet visible absorption spectra were measured using a V550 spectrophotometer (JASCO) as described previously.[25,26] Spectral changes accompanying the regeneration of dark state (D450 state) from light state (S390 state) were monitored after BL illumination (λ_{max} at 470 nm for 1 min) at 25°C in the dark. The regeneration curves were obtained from the absorbance at 450 nm. Each absorbance difference curve was fitted by a single exponential expression using the formula, $\Delta A_{max}(1-e^{-kt})$, where ΔA_{max} was the maximum

Please do not adjust margins

absorbance difference and k was the rate constant of regeneration. Fluorescence emission spectra were measured at 25°C with excitations at 510 nm (for YFP-fused PZs) and 570 nm (for mCh-fused PZs) using an F-7000 fluorescence spectrophotometer (Hitach HiTech).

DLS measurements

DLS of the protein solutions were measured with a Zetasizer-μV system (Mavern Instruments) in automatic mode at 25°C, and the z-average molecular sizes expressed as $R_{H(app)}$ in solution were determined using Zetersizer Software (version 6.20) as previously described.[25-27] Briefly, the stock protein solutions were diluted to 5-8 μM with the loading buffer. After removing the aggregates by centrifugation, light scattering was detected using a solution refractive index of 1.334, and the viscosity of the loading buffer (0.9166×10^{-3} pascal·s^{-1}). DLS of the recombinant proteins was measured several times in the dark (dark state), and immediately after the termination of BL illumination for 1 min (light state). For measuring DLS in the light-dark state, illuminated samples were incubated for 1 h in the dark after illumination. $R_{H(app)}$ of samples was plotted versus the concentration, and R_H values were obtained from the extrapolated values at 0 μM protein concentration.[25-27] In these experiments, DLS data resulting in a polydispersity index larger than 0.3 were omitted. Standard deviations of all $R_{H(app)}$ values obtained from the multiple measurements were less than 0.05 nm.

SEC measurements

SEC was performed using an AKTA purifier column chromatography system (GE Healthcare) with a Superdex S−200 30/10 column (GE Healthcare), using an SEC buffer containing 300 mM (for C-fusion PZs) and 230 mM (for N-fusion PZs) NaCl and 20 mM Tris-HCl (pH 7.0) at 25 ± 1°C, with a flow rate of 0.5 mL/min.[26,27] All sample solutions were incubated for 20 min at 25°C in the dark, and 250 μL aliquots containing 2 μM protein were used for analyses (dark state). Sample solutions were illuminated for 1 min with BL, and applied to the column continuously illuminated with a LED light (light state). BL-illuminated samples were kept in the dark for 1 h to measure the light-dark state. For molecular mass calibration of the recombinant proteins, spherical proteins in gel filtration calibration kits (GE Healthcare) were used as size markers; these included ribonuclease A (13.7 kDa), carbonic anhydrase (29 kDa), ovalbumin (43 kDa), conalbumin (75 kDa), aldolase (158 kDa), ferritin (440 kDa), and thyroglobulin (669 kDa), using a column volume of 24 mL and a void volume of 8 mL.

Notes and References

1. J. M. Christie, *Annu. Rev. Plant Biol.*, 2007, **58**, 21-45.
2. T. Imaizumi, H. G. Tran, T. E. Swartz, W. R. Briggs, and S. A. Kay, *Nature*, 2003, **426**, 302-306.
3. M. Avila-Pérez, J. Vreede, Y. Tang, O. Bende, A. Losi, W. Gärtner and K. Hellingwerf, *J. Biol. Chem.*, 2009, **284**, 24958-24964.
4. T. E. Swartz, T. Tseng, M. A. Frederickson, G. Paris, D. J. Comerci, G. Rajashekara, J.-G. Kim, M. B. Mudgett, G. A. Splitter, R. A. Ugalde, F. A. Goldbaum, W. R. Briggs, R. A. Bogomolni, *Science*, 2007, **317**, 1090-1093.
5. E. B. Purcell, D. Siegal-Gaskins, D. C. Rawling, A. Fiebig, and S. S. Crosson, *Proc. Natl. Acad. Sci. USA*, 2007, **104**, 18241-18246.
6. E. B. Djouani-Tahr, J. M. Christie, S. Sanchez-Ferandin, F. Sanchez, F. Y. Bouget and F. Corellou, *Plant J.*, 2011, **65**, 578-588.
7. M. Salomon, J. M. Christie, E. Kneib, U. Lempert and W. R. Briggs, *Biochemistry*, 2000, **39**, 9401-9410.
8. T. E. Swartz, S. B. Corchnoy, J. M. Christie, J. W. Lewis I., Szundi, W. R. Briggs and R. A. Bogomolni, *J. Biol. Chem.*, 2001, **276**, 36493-36500.
9. T. Iwata, S. Tokutomi and H. Kandori, *J. Am. Chem. Soc.*, 2002, **124**, 11840-11841.
10. J. Lee, M. Natarajan, V. C. Nashine, M. Socolich, T. Vo, W. P. Russ, S. J. Benkovic, R. Ranganathan, *Science*, 2008, **322**, 438–442.
11. M. Yazawa, A. M. Sadaghiani, B. Hsueh, R. E. Dolmetsch, *Nat. Biotechnol.*, 2009, **27**, 941–945.
12. Y. I. Wu, D. Frey, O. I. Lungu, A. Jaehrig, I. Schlichting, B. Kuhlman and K. M. Hahn, *Nature*, 2009, **461**, 104–108.
13. U. Krauss, J. Lee, S. J. Benkovic and K. E. Jaeger, *Microb. Biotechnol.*, 2010, **3**, 15–23.
14. A. Moglich, R. A. Ayers and K. Moffat, *J. Mol. Biol.*, 2010, **400**, 477–486.
15. X. Wang, X. Chen and Y. Yang, *Nat. Methods*, 2012, **9**, 266-269.
16. D. Strickland, Y. Lin, E. Wagner, C. M. Hope, J. Zayner, C. Antoniou, T. R. Sosnick, E. L. Weiss and M. Glotzer, *Nat. Methods*, 2012, **9**, 379–384.
17. L. R. Polstein and C. A. Gersbach, *J. Am. Chem. Soc.*, 2012, **134**, 16480-16483.
18. O. I. Lungu, R. A. Hallett, E. J. Choi, M. J. Aiken, K. M. Hahn and B. Kuhlman, *Chem Biol.*, 2012, **19**, 507-517.
19. C. Renicke, D. Schuster, S. Usherenko, L. O. Essen and C. A. Taxis, *Chem Biol.*, 2013, **20**, 619-626.
20. F. Takahashi, D. Yamagata, M. Ishikawa, Y. Fukamatsu, Y. Ogura, M. Kasahara, T. Kiyosue, M. Kikuyama, M. Wada and H. Kataoka, *Proc. Natl. Acad. Sci. USA*, 2007, **104**, 19625-19630.
21. M. Ishikawa, F. Takahashi, H. Nozaki, C. Nagasato, T. Motomura and H. Kataoka, *Planta*, 2009, **230**, 543-552.
22. E. Malzahn, S. Ciprianidis, K. Káldi, T. Schafmeier and M. Brunner, *Cell*, 2010, **142**, 762-772.

8 | *Photochem. Photobiol. Sci.*, 2015, **00**, 1-6

This journal is © The Royal Society of Chemistry 20xx

23 A. I. Nash, R. McNulty, M. E. Shillito, T. E. Swartz, R. A. Bogomolni, H. Luecke and K. H. Gardner, *Proc. Natl. Acad. Sci. USA*, 2011, **108**, 9449– 9454.

24 T. E. Ellenberger, C. J. Brandl, K. Struhl and S. C. Harrison, *Cell*, 1992, **71**, 1223-1237.

25 T. Toyooka, O. Hisatomi, F. Takahashi, H. Kataoka and M. Terazima, *Biophys. J.*, 2011, **100**, 2801-2809.

26 O. Hisatomi, K. Takeuchi, K. Zikihara, Y. Ookubo, Y. Nakatani, F. Takahashi, S. Tokutomi and H. Kataoka, *Plant Cell Physiol.*, 2013, **54**, 93–106.

27 O. Hisatomi, Y. Nakatani, K. Takeuchi, F. Takahashi and H. Kataoka, *J. Biol. Chem.*, 2014, **289**, 17379-17391.

28 C. Duellberg, M. Trokter, R. Jha, I. Sen, M. O. Steinmetz and T. Surrey. *Nature Cell Biol.*, 2014, **16**, 8, 804-8011.

29 K. Takeuchi, Y. Nakatani and O. Hisatomi, *Open J. Biophys.*, 2014, **4**, 83-91.

30 W. Liptay, *Angew. Chem. internat. Edit.*, 1969, **8**, 177–188.

31 A. Möglich and K. Moffat, *Photochem Photobiol Sci.*, 2010, **9**, 1286-1300.

32 Y. Nakatani and O. Hisatomi, *Biochemistry*, 2015, **54**, 3302-3313.

33 Y. Nihongaki, H. Suzuki, F. Kawano and M. Sato, *ACS Chem Biol.*, 2014, **9**, 617-621.

34 L. B. Motta-Mena, A. Reade, M. J. Mallory, S. Glantz, O. D. Weiner, K. W. Lynch and K. H. Gardner, *Nat. Chem. Biol.*, 2014, **10**, 196-202.

35 F. Kawano, H. Suzuki, A. Furuya, M. Sato, *Nat Commun.*, 2015, **6**, 6256.

36 M. Grusch, K. Schelch, R. Riedler, E. Reichhart, C. Differ, W. Berger, A. Ingles-Prieto and H. Janovjak, *EMBO J.*, 2014, **33**, 1713–1726.

A graphical and textual abstract for the Table of contents entry (Hisatomi and Furuya)
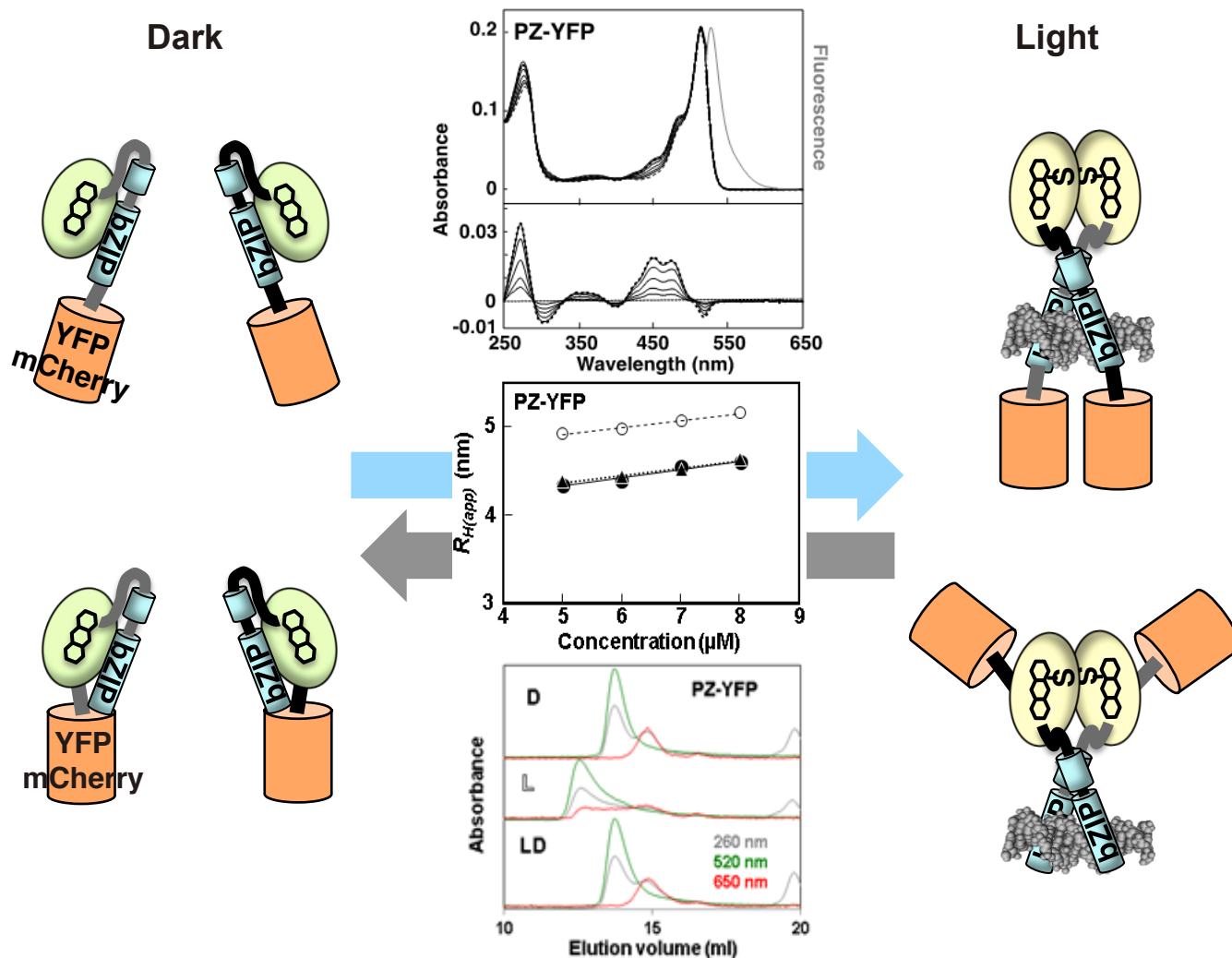
Yellow fluorescent protein or mCherry protein fused with the Photozipper underwent blue light-induced dimerization, which enhanced their affinities for the target DNA.